



Involvement of *B-aat1* and *Cbs* in regulating mantle pigmentation in the Pacific oyster (*Crassostrea gigas*)

Zhuanzhan Li¹ · Biyang Hu¹ · Lijie Du¹ · Chunhao Hou¹ · Qi Li^{1,2}

Received: 5 July 2022 / Accepted: 17 October 2022 / Published online: 6 November 2022
© The Author(s), under exclusive licence to Springer Nature B.V. 2022

Abstract

Background Shell color formation is an important physiological process in bivalves, the molecular genetic basis has potential application in bivalve aquaculture, but there is still remaining unclear about this issue. The cystine/glutamate transporter (*Slc7a11*) and cystathionine beta-synthase (*Cbs*) are integral genes in pheomelanin synthesis pathway, which is vital to skin pigmentation.

Methods and results Here, the sequences of b (0, +)-type amino acid transporter 1 (*B-aat1*) and *Cbs* in Pacific oyster (*Crassostrea gigas*) (*CgB-aat1*, *CgCbs*) were characterized. Phylogenetically, the deduced amino acid sequences of *CgB-aat1* and *CgCbs* both possessed conserved features. Genes were both ubiquitously expressed in six tested tissues with more abundant expression level in central mantle. Besides, the polyclonal antibodies of *CgB-aat1*, *CgCbs*, *CgTyr*, and *CgTyrp2* were successfully prepared. Immunofluorescence analysis revealed that *CgB-aat1* and *CgCbs* proteins were both expressed in gill rudiments of eyed-larvae and concentrated mainly in cytoplasm of epithelial cell and nerve axons in mantle. Additionally, after *CgB-aat1* or *CgCbs* silencing, expressions at mRNA and protein levels of *CgB-aat1* and *CgCbs* involved in pheomelanin synthesis were significantly suppressed, and *CgTyr*, *CgTyrp1* and *CgTyrp2* related to eumelanin synthesis were also down-regulated but no apparent differences, respectively. Moreover, micrographic examination found less brown-granules at mantle edge in *CgB-aat1* interference group.

Conclusion These results implied that pheomelanin synthesis was possible induced by *CgB-aat1*-*CgTyr*-*CgCbs* axis, and it played an essential role on mantle pigmentation in the oysters. These findings provide the useful genetic knowledge and enrich the physiological information for the shell color formation in bivalve aquaculture.

Keywords *B-aat1* · *Cbs* · RNA interference · Melanin granules · *Crassostrea gigas*

Abbreviations

<i>B-aat1</i>	B (0, +)-type amino acid transporter 1
<i>Cbs</i>	Cystathionine beta-synthase
<i>Eflα</i>	α Subunit of elongation factor 1
HPLC	High-performance liquid chromatography
HRP	Horseradish peroxidase
IF	Immunofluorescence
IPTG	Isopropyl β-D-thiogalactoside
<i>Mitf</i>	Microphthalmia-associated transcription factor

<i>Pax3/7</i>	Paired box 3/7
<i>Slc7a11</i>	Solute carrier family 7 member 11 (xCT)
SDS-PAGE	Sodium dodecyl sulfate polyacrylamide gel electrophoresis
<i>Tyr</i>	Tyrosinase
<i>Tyrp1</i>	Tyrosinase-related protein 1
<i>Tyrp2</i>	Tyrosinase-related protein 2
WB	Western blot

Introduction

The colorful molluscan shells are widely recognized and have been appreciated by collectors and scientists. Colorful shell is mainly because of the biological pigments. Melanin, one of the most common pigments, include black eumelanin (brown/black pigment) and lighter pheomelanin (orange/red pigment). Both of them was found in

✉ Qi Li
qili66@ouc.edu.cn

¹ Key Laboratory of Mariculture, Ministry of Education, Ocean University of China, Qingdao 266003, China

² Laboratory for Marine Fisheries Science and Food Production Processes, Qingdao National Laboratory for Marine Science and Technology, Qingdao 266237, China

mammals, birds and insects, and only eumelanin was found in fish [1]. However, melanin in molluscan shells has not been fully characterized due to the fact that it is difficult to isolate [2]. Until now, Affenzeller et al. [3] found the existence of pheomelanin in the terrestrial gastropod *Cepaea nemoralis* using HPLC.

In addition, the biosynthetic and molecular pathway of melanin synthesis are well not understood in mollusks, except in insects and mammals [1, 4]. Generally, *Tyr* initiates eumelanogenesis by hydroxylating tyrosine to dopa and oxidizing the resultant dopa to dopaquinone, which is then converted to eumelanin polymer by *Tyrp1* and *Tyrp2* [5]. On the other hand, *SLC7a11/xCT* can transport cystine into cell. Subsequently, cystine and dopaquinone are catalyzed by CBS and consequently promote the synthesis of pheomelanin [1, 6]. Recently, omics analysis in different color varieties of fishes have been done to confirm the conserved melanogenesis pathway in fish [7–9]. Furthermore, the sequences, expressions and functions of *Slc7a11/xCT* involved in skin color have been characterized in vertebrate [10–13]. And the structural characterize of *Cbs* is also well studied that has crucial role in transsulfuration for cysteine biosynthesis [14]. These works demonstrated that *Slc7a11/xCT* and *Cbs* act vital roles in pheomelanin synthesis pathway. To date, the complete pathway of melanin synthesis in mollusks is not known, several genes such as *Tyr*, *Tyrp2*, *Mitf* and *Pax3/7* have been shown to be important in the regulation and production of melanin in mollusks [15–17]. However, other research on molecular pathway of pheomelanin synthesis in mollusks are still poorly understood and no study to date has addressed these issues.

The Pacific oyster, *Crassostrea gigas*, is one of the most economically important marine bivalve species. Recently, oysters with orange shell both of the right and left, a recessive trait compared to black and white, were obtained from breeding program [18]. The whole transcriptome analysis revealed that melanin biosynthesis-related genes functioned on orange shell coloration in *C. gigas* [19]. Currently, existing research was limited to quantification of melanin synthesis related genes in *C. gigas*. Hence, it is urgent to study the molecular characteristics and function in shell color of these genes.

Here, *B-aat1* and *Cbs* gene from orange shell color oysters were characterized and expressed. Furthermore, gene function was deliberated by RNAi technology, one of the methods of transporting dsRNA was bacterial feeding, which has been well applied in *C. gigas* [20, 21]. These results will help understand the overall role of *B-aat1* and *Cbs* in pheomelanin synthesis pathway and mantle pigmentation as well as advance our knowledge of shell color genetics in bivalve.

Materials and methods

Oysters collection

The Pacific oyster is neither an endangered nor protected species. All experiments in this study were conducted according to national and institutional guidelines. Here, one-year old oysters with orange shell color were supplied with filtered seawater at ambient temperature (24 ± 1 °C), salinity (30.5 ± 0.5 psu) and pH (8.1), which was the same with condition in farm of Rongcheng, Shandong province, China. Seven days later, the oysters (shell length 24.02 ± 8.09 cm and shell height 36.55 ± 9.08 cm) were chosen for sampling. Six tissues, including digestive gland, labial palp, gill, mantle edge, central mantle, and adductor muscle were dissected and immediately stored at -80 °C for RNA extraction. In embryonic and larval sampling, oysters with orange shell color were transported to Litao hatchery, Yantai City, Shandong Province. The embryos were obtained following our previous study [21]. In brief, after mixing sperm and oocytes, fertilized eggs were reared with temperature (23 – 25 °C) and salinity (30 – 31 psu). *Isochrysis galbana* and *Chaetoceros calcitrans* were mixed to feed larvae daily. In a month, fertilized egg, blastula, gastrula, trochophore, D-shaped larvae 1/2, umbo larva 1/2 and eyed-larva were collected for RNA extractions and IF analysis.

Bioinformatics analysis

The amino acid (aa) sequences of b (0, +) -type amino acid transporter 1 (*B-aat1*) and cystathionine beta-synthase (*Cbs*) in *C. gigas* (*CgB-aat1*, XP_034337681.1; *CgCbs*, XP_034300359.1) and *B-aat1/Slc7a11* as well as *Cbs* from other organisms were retrieved from NCBI database (Table 1). The SMART database (<http://smart.embl-heidelberg.de/>) was used to predict gene function domain. The TMHMM-2.0 database (<https://services.healthtech.dtu.dk/service.dtu.dk/service.php?TMHMM-2.0>) was used to analysis transmembrane helices of *CgB-aat1* protein. Multiple sequence alignment of *CgB-aat1* and *CgCbs* proteins with other known *B-aat1/Slc7a11* and *Cbs* proteins was performed using DNAMAN 8.0 software. The alignment of the sequences was analyzed using Clustal X 2 and phylogenetic tree was constructed with the method of maximum-likelihood algorithm using MEGA X.

Gene expression analysis

The cDNA template used for qPCR was synthesized using PrimeScript™ RT reagent Kit (Takara, China). The Primer3 from NCBI (<https://www.ncbi.nlm.nih.gov/tools/>

Table 1 The *B-aat1/Slc7a11* and *Cbs* genes information used for phylogenetic analysis

No	Organism name	Protein name (Gene name)	Accession Number
1	<i>Crassostrea gigas</i>	B (0, +)-type amino acid transporter 1 (B-aat1) Cystathionine beta-synthase (Cbs)	XP_034337681.1 XP_034300359.1
2	<i>Crassostrea virginica</i>	B (0, +)-type amino acid transporter 1-like isoform X1 (B-aat1) Cystathionine beta-synthase-like (Cbs)	XP_022344420.1 XP_022322044.1
3	<i>Mytilus coruscus</i>	Cystathionine beta-synthase (Cbs)	CAC5416117.1
4	<i>Mizuhopecten yessoensis</i>	B (0, +)-type amino acid transporter 1-like (B-aat1) Cystathionine beta-synthase-like isoform X1 (Cbs)	XP_021347059.1 XP_021364962.1
5	<i>Mytilus galloprovincialis</i>	Cystathionine beta-synthase (Cbs)	VDI56218.1
6	<i>Haliotis rufescens</i>	B (0, +)-type amino acid transporter 1-like (B-aat1) Cystathionine beta-synthase-like isoform X3 (Cbs)	XP_046364599.1 XP_046332497.1
7	<i>Pecten maximus</i>	B (0, +)-type amino acid transporter 1-like isoform X2 (B-aat1) Cystathionine beta-synthase-like isoform X2 (Cbs)	XP_033753742.1 XP_033757822.1
8	<i>Sepia pharaonis</i>	Cystathionine beta-synthase (Cbs)	CAE1265012.1
9	<i>Oreochromis mossambicus</i> × <i>niloticus</i>	Solute carrier family 7 member 11 transcript variant 1 (Slc7a11)	QDK64624.1
10	<i>Danio rerio</i>	cystine/glutamate transporter (Slc7a11) Cystathionine beta-synthase (Cbs)	XP_009289503.1 AAW78657.1
11	<i>Mus musculus</i>	cystine/glutamate transporter (Slc7a11) Cystathionine beta-synthase (Cbs)	NP_036120.1 AAH26595.1
12	<i>Xenopus laevis</i>	cystine/glutamate transporter (Slc7a11) Cystathionine-beta-synthase S homeolog (Cbs)	XP_018098795.1 NP_001086820.1
13	<i>Gallus gallus</i>	cystine/glutamate transporter isoform X1(Slc7a11) Cystathionine beta synthase (Cbs)	XP_426289.3 VTO94514.1
14	<i>Homo sapiens</i>	cystine/glutamate transporter (Slc7a11) Cystathionine beta synthase (Cbs)	NP_055146.1 VTO94514.1

primer-blast/) was used to design qPCR primer pairs (listed in Table S1), in which *ef1a* gene was set as reference gene [22]. The qPCR reactions were performed with QuantiNova™ SYBR® Green PCR Kit (QIAGEN, Germany) on LightCycler 480 real-time PCR instrument (Roche, Switzerland). Three repeats of each cDNA sample were reacted in 10 µL volume, respectively, which contained 5 µL 2× SYBR Green PCR Master Mix, 1 µL cDNA template, 2 µL ddH₂O and 1 µL each 10 mM primer. The PCR reaction were as follows: 95 °C for 2 min, followed by 40 cycles of 95 °C for 5 s and 60 °C for 10 s. All primers specificity were confirmed by melt curve (65–95 °C) analysis. The $2^{-\Delta\Delta CT}$ method was applied to gene expression analysis [23]. All data were shown as means ± standard error (SE) (n = 6). Statistically significant differences were analyzed using *t*-test and one-way ANOVA method between two data and among multiple data, respectively. The significance level was considered at $P < 0.05$.

Antibody preparation and WB examination

The recombinant *CgCbs*, *CgTyr* and *CgTyrp2* protein was generally conducted respectively as described by Liu et al.

[24]. For *CgB-aat1*, we generated the antibody again rabbit polyclonal antibody from a 11-residue polypeptide (CGE-PQIPKKMI). The other purified *CgCbs*/ *CgTyr*/ *CgTyrp2* recombinant protein was used to immunize two rabbits. In brief, four immunizations were performed at 8 days intervals. After immunization twice, antiserum collection and ELISA assay was conducted weekly to assess the immunity level. Following the titer evaluation, antibody specificity was verified by WB as described below.

Purified proteins and antibody obtained were detected using WB. In details, recombinant proteins (20 µg) were separated on 12.5% (v/v) polyacrylamide vertical slab gel and transferred onto polyvinyl difluoride membrane (Beyotime, Shanghai, China). Following blocking with 5% skimmed milk at 25 °C for 2 h, the membrane was incubated with His-tag (Beyotime, China) /*CgB-aat1*/*CgCbs*/*CgTyr*/*CgTyrp2* polyclonal antibody (diluted 1:2000 in Blocking Solution) at 4 °C overnight and then incubated with HRP-conjugated goat anti-rabbit IgG (Beyotime, China) at 37 °C for 2 h. The chemiluminescence reaction was performed using the enhanced ECL chemiluminescence reaction detection kit (Vazyme, China) and protein bands were imaged with Gel Image System (JS-2000).

Immunofluorescence

IF examinations of *CgB-aat1* and *CgCbs* proteins in eyed-larva and mantle tissue were performed according to the description by Wang et al. [10] with some modifications. Simply, the mantle was treated with fixation in Bouin reagent, dehydration in ethanol, transparent in xylol, embedding in paraffin and section in 5 μm thickness. Then, the slices were incubated in 0.01 M citrate buffer (pH=6) at 100 °C for 10 min for antigen retrieval. After blocking with 7.5% goat serum (Beyotime), the primary antibody (anti-*CgB-aat1* antibody with 1:1000 dilution and anti-*CgCbs* antibody with 1:500 dilution) incubation was performed at 4 °C overnight, then the samples were hatched with Alexa fluor® 488-labeled Goat Anti-Rabbit secondary antibody (1:500 dilution, cat. nos. A0423, Beyotime) at room temperature for 90 min. The normal goat serum incubation was set as the negative control. Cell nuclei were counterstained with DAPI (Beyotime). Finally, samples were captured using confocal microscopy (TCS SP98, Leica, Germany).

Synthesis and feeding of dsRNA

The fragments of *CgB-aat1* and *CgCbs* genes were produced by PCR with primers listed in Table S1. Sub-cloning, ligation, transfection and induced expression were used for dsRNA synthesis base on the detailed description by Feng et al. [20]. Here, after transformation with three constructed plasmids (*CgB-aat1*-L4440, *CgCbs*-L4440 and *EGFP*-L4440), respectively, bacteria (*Escherichia coli* strain HT115) were induced by IPTG for producing three dsRNAs, respectively. *EGFP* was used as a negative control (NC). The non-induced *E. coli* and IPTG-induced *E. coli* transformed were collected for RNA isolation using Bacteria RNA Extraction Kit (Vazyme, China), respectively.

One-year-old oysters with orange shell were used for dsRNA feeding experiment after acclimating for 10 days at the same environment mentioned in Part 2.1. In which, oysters with shell length of 23.67 ± 8.03 cm and shell height of 33.75 ± 7.64 cm were selected. In this study, ten oysters in *CgB-aat1*-RNAi group, *CgCbs*-RNAi group and EGFP-RNAi group were carried out, respectively. During the feeding period, bacteria (*E. coli* strain HT115) containing recombinant plasmid were cultivated in LB medium at 37 °C overnight. The bacteria were diluted 100-fold in 500 mL medium and cultured until the OD₅₉₅ values reached 0.4. Subsequently, 0.4 mM IPTG was added and incubated for 4 h to induce dsRNA production. Bacterial pellets obtained were re-suspended in 500 mL *Platymonas subcordiformis* and 125 mL *Nitzschia closterium f. minutissima* algae culture liquid. Then, oysters were fed with 625 mL Alga/dsRNA-producing bacteria co-inoculum once a day and fed with only alga twice a day. The 60% of seawater volume

was changed daily with aerated seawater (24 ± 1 °C). After 40 days feeding, the dead oyster was not observed and mantles collected were used for RNA extraction, gene and protein expressions and histology examination.

Protein expression in mantle of *CgB-aat1*-RNAi group, *CgCbs*-RNAi group and EGFP-RNAi group (denoted as B-aat1-i, Cbs-i and Egfp-i, respectively) were analyzed using WB. In detail, the mantles were homogenized in 1×PBS buffer and centrifuged at 13,000 *g* for 15 min, then the supernatants collected was used to measure the protein concentration using the Nanodrop 2000 (Thermo scientific, USA) [25]. Protein with 20 μg was prepared for loading, which was carried out as described above. The GAPDH rabbit monoclonal antibody diluted 1000-fold was served as control. *CgB-aat1*, *CgCbs*, *CgTyr*, *Tyrp1* (abcam ID: EPR21956) and *CgTyrp2* polyclonal antibody were used to detected the corresponding protein expression level in three groups, respectively.

Histology analysis

Mantle tissues from oysters in three groups were sampled after RNAi experiment and were used for analyzing histological structure changes of mantle. The slices of mantle were obtained following the method mentioned in IF. Then the sections were stained with H&E and examined under an Olympus BX53 light microscope (Olympus Corporation, Japan).

Results

Identifications of *CgB-aat1* and *CgCbs* protein

In the deduced 497 aa *CgB-aat1* protein, ten transmembrane regions were predicted using TMHMM-2.0 database (Fig. S1). The deduced aa sequences of *CgB-aat1* and *CgCbs*, both possess conserved features among multiple species (Fig. S2a, c). Phylogenetic analysis showed that *CgB-aat1* clusters together with sequences from other mollusks, finally with vertebrates (Fig. S2b). Phylogenetic analysis of *CgCbs* revealed all *Cbs* genes were classified into two clusters, *Cbs* genes in vertebrates and invertebrates were classified to a big clade, respectively (Fig. S2d).

Expressions of *CgB-aat1* and *CgCbs*

The expression of *CgB-aat1* gene have distinct expression pattern in embryo-larval stages, significant increase of *CgB-aat1* gene expression was detected at D-shaped 1 stage, where the expression upped to the top ($P < 0.05$) (Fig. 1a). The mRNA level of *CgB-aat1* gene was widely distributed in six tissues, in which the highest expression

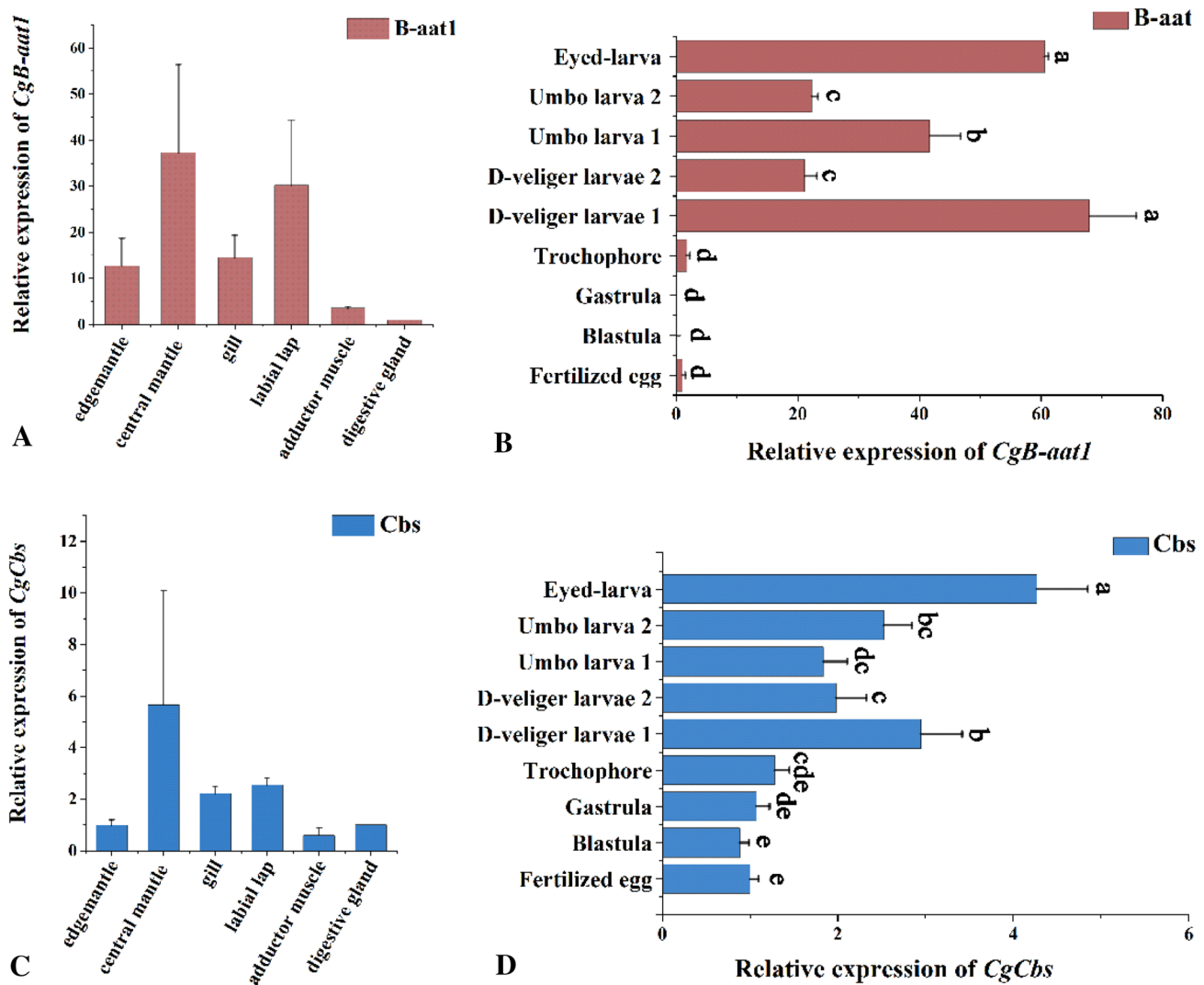


Fig. 1 Expression analysis of *CgB-aat1* and *CgCbs* genes estimated by qPCR. **a, c** Gene expression profiles of *CgB-aat1* (**a**) and *CgCbs* (**c**) in six tissues. The digestive gland tissue was set as control. **b, d** Gene expression profiles of *CgB-aat1* and *CgCbs* during embryonic

and larval development. The fertilized egg was set as control. The significant difference ($P < 0.05$) was shown with different letters and all data were shown as mean \pm standard error (SE) ($n = 6$)

was detected in central mantle, the lowest was in digestive gland (Fig. 1b). The results showed that *CgCbs* gene was also mainly expressed in eyed-larva ($P < 0.05$), with lower expression in the period before the blastula stage ($P < 0.05$) (Fig. 1c). *CgCbs* gene was also ubiquitously expressed in adult six tissues investigated with more abundant expression level in central mantle (Fig. 1d).

Prokaryotic expression and antibody preparation

The expression of *CgCbs/CgTyr/CgTyrp2* recombinant protein was successfully induced by IPTG in *E. coli* BL21 (DE3), SDS-PAGE result indicated that the target band migrated at about 18 kDa, 25 kDa, 20 kDa, respectively (line 3 in Fig. 2a, b, c, respectively). Purified recombinant

CgCbs, *CgTyr* and *CgTyrp2* proteins revealed a single band, respectively, and located at predicted molecular mass range (Fig. S3a–c). Purified protein was confirmed by WB, the result showed that purified protein with N-terminal His tag was specific to Rabbit anti-His-tag antibody (Fig. S3d). Polyclonal *CgCbs/CgTyr/CgTyrp2* antibody was produced by immunizing rabbit with recombinant *CgCbs/CgTyr/CgTyrp2* protein and the binding relationship with antigen was monitored by WB. After the specific antibody against the *Cbs/Tyr/Tyrp2* fusion protein, a single band at around 18 kDa (Fig. 2d) / 25 kDa (Fig. 2e) / 20 kDa (Fig. 2f) was detected, respectively. Additionally, the specificity of *Tyrp1* monoclonal antibody in mantle of *C. gigas* was confirmed by IF pretest (data not shown).

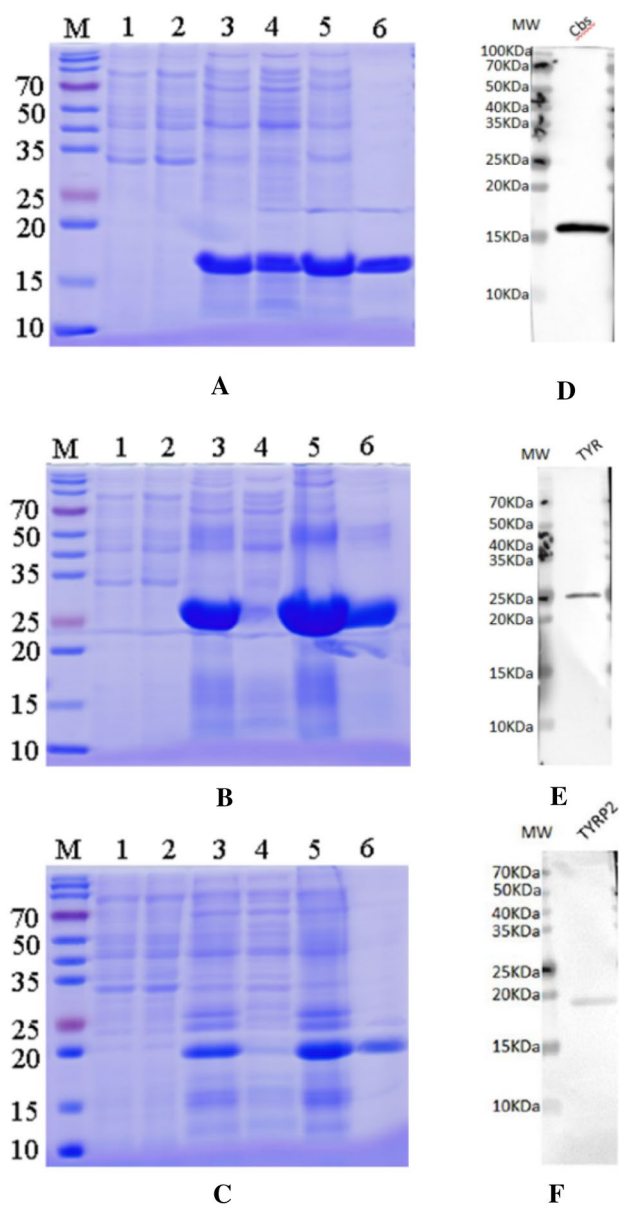


Fig. 2 Production of recombinant *CgCbs*, *CgTyr* and *CgTypr2* proteins as well as WB validation of the antibodies. Determination of expression and purification of recombinant *CgCbs* (a), *CgTyr* (b) and *CgTypr2* (c) protein by SDS-PAGE analysis. M, molecular marker; Lane 1, BL21 without recombinant plasmid; Lane 2, protein expressed without IPTG induction (used as a negative control); Lane 3, protein expressed with IPTG induction for 6 h; Lane 4, soluble protein of supernatant; Lane 5, inclusion body; Lane 6, purified recombinant protein. The specificity of the *CgCbs* (d), *CgTyr* (e) and *CgTypr2* (f) antibody was verified by WB, respectively

Localization of *CgB-aat1* and *CgCbs* proteins

IF analysis in eyed-larvae showed that *CgB-aat1* protein mainly located in mantle and gill rudiments [Fig. 3a (b1–b2)]. And positive signals of anti-Cbs were observed in gill rudiments and anterior adductor muscle [Fig. 3a

(c1)]. IF analysis results in mantle showed green fluorescence was mainly distributed on the cytoplasm of epithelial cell and nerve axons, indicating that *CgB-aat1* and *CgCbs* proteins are mainly located on the cytoplasm in this organ (Fig. 3b). There was no signal was found in control groups conducted in both of eyed-larvae [Fig. 3a (d)] and mantle tissues [Fig. 3b (b1–b3)].

Expressions of *CgB-aat1* and *CgCbs* were inhibited after RNA interference

Gene expressions levels of *CgB-aat1* and *CgCbs* genes were reduced by 97.52% in *CgB-aat1* dsRNA group (Fig. 4a) and 63.46% in *CgCbs* dsRNA group ($P < 0.05$) in comparison with EGFP dsRNA group (negative control, NC), respectively (Fig. 4b). WB results displayed that *CgB-aat1/CgCbs* protein was obvious depressed when compared with NC group (Fig. 4c). There was no doubt that *CgB-aat1/CgCbs* dsRNA feeding could effectively inhibit *CgB-aat1/CgCbs* expression.

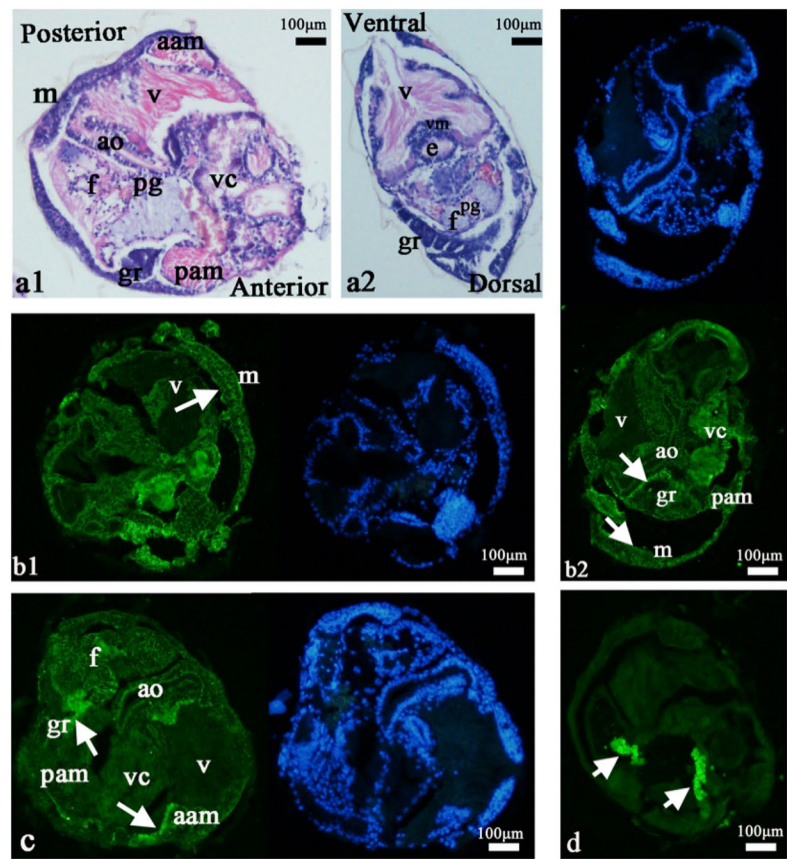
Effect of *CgB-aat1* and *CgCbs* silencing on the expression of the key genes associated with melanin synthesis

The expression differences of *CgCbs* and key genes associated with melanin synthesis, *CgTyr*, *CgTypr1* and *CgTypr2* genes were analyzed by qPCR after the downregulation of *CgB-aat1/CgCbs*. As shown in Fig. 4a, b, *CgCbs*, participating in the intermediate process of pheomelanin synthesis, its expression was also decreased by 74.76% ($P < 0.05$) after *CgB-aat1* silencing. And there was no significant change of *CgB-aat1* gene expression in *CgCbs* interference group. *CgTyr* played a vital role in catalyzing melanin synthesis and its transcriptional level was significantly declined by 83.93% ($P < 0.05$) in *CgCbs* dsRNA feeding. However, no significant difference was observed after *CgB-aat1* silencing. *Typr1* and *Typr2* were functioned in melanocyte migration and differentiation, *CgTypr1* and *CgTypr2* gene expression were also no obvious difference after *CgTypr1* and *CgTypr2* knock-down, respectively. The same phenomenon was occurred in corresponding protein expression (Fig. 4c).

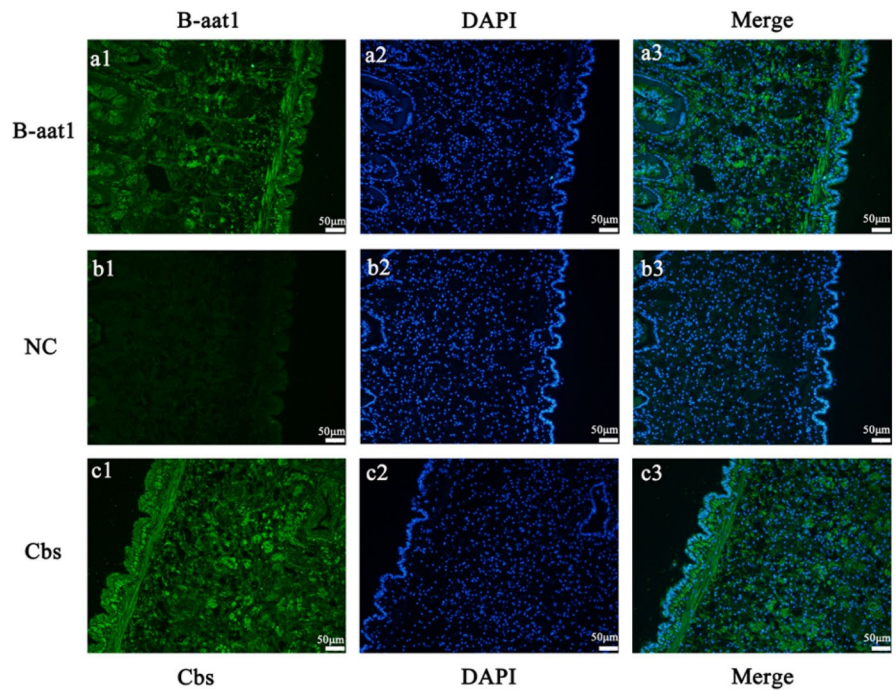
Histology changes of mantle after RNA interference

The effects of *CgB-aat1* and *CgCbs* silencing on histological features of mantle were displayed in Fig. 5. Compared with NC group, brown-granule in the epithelial tissue of mantle was decreased in *CgB-aat1* interference group (Fig. 5a). However, there was no obvious changes of melanin granules of mantle between *CgCbs* interference group and NC group.

Fig. 3 IF localization of *CgB-aat1* and *CgCbs* proteins in eyed-larva (a) and in the mantle (b). **a** IF of competent eyed-larvae sections for *CgB-aat1* and *CgCbs* protein (green fluorescence). The blue fluorescence is nucleus (N). Each fluorescent IF section is accompanied with section stained with H&E technique (a1–a2). aam: anterior adductor muscle; ao: apical organ; f: foot; gr: gill rudiments; m: mantle; pam: posterior adductor muscle; pg: pedal ganglion v: vellum with cilia; vc: visceral cavity; vm: vellum membrane. **b1–c1** Sagittal section of whole competent larvae. Scale bar = 100 μ m. **b1–b2** Obvious positive signals of anti-*CgB-aat1* were observed in mantle (m shown with white arrow in b1), gill rudiments (gr shown with white arrows in b2). The false positive was shown in the around of the visceral cavity. **c1** Sagittal section of whole competent larvae. Stronger positive signals of anti-*CgCbs* were shown in gill rudiments and anterior adductor muscle, showing with white arrows. **d1** Immunofluorescence localization analyses in negative control. The negative controls (NC) were incubated with normal goat serum. The white arrows mean false positive. **b** Positive signals of anti-*CgB-aat1* and anti-*CgCbs* immunolabeling were shown in green fluorescence (a1, c1), which was mainly distributed on the cytoplasm of epithelial cell and nerve axons in mantle. The blue fluorescence is nucleus (N) (a2, c2). The negative controls (NC) were incubated with normal goat serum and there was no obvious positive signal observed in NC group. Scale bar = 100 μ m. (Color figure online)



A



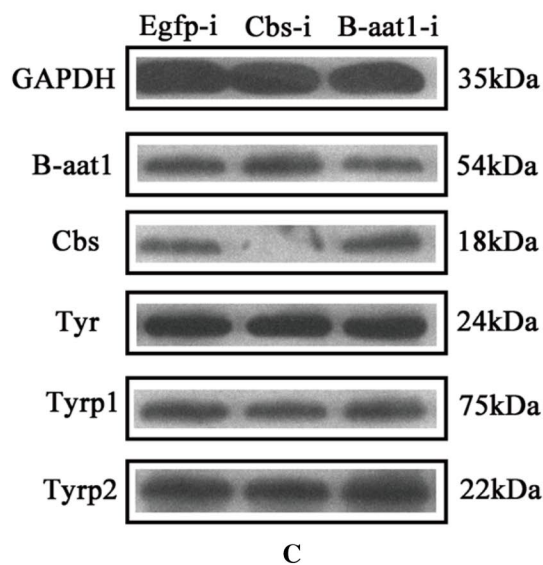
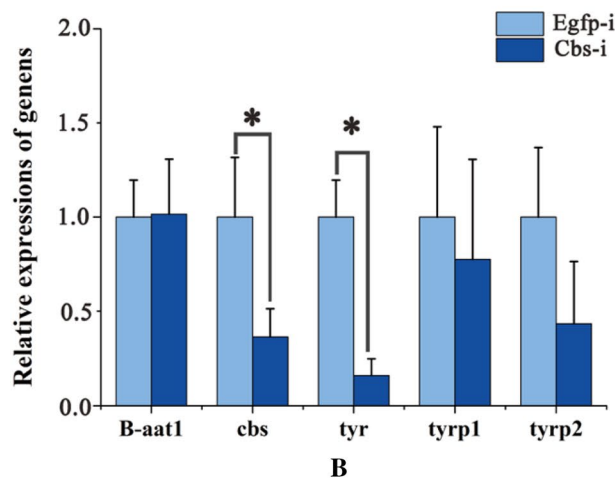
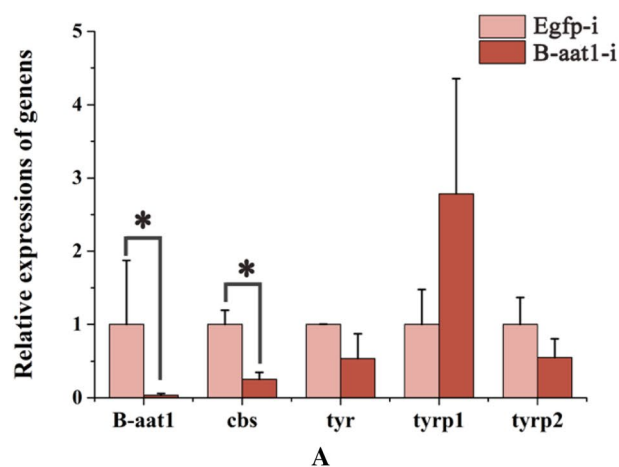
B

Fig. 4 Expressions of *CgB-aat1*, *CgCbs*, *CgTyr*, *CgTyrp1* and *CgTyrp2* after *CgB-aat1* and *CgCbs* silencing, respectively. **a, b** Gene expressions of *CgB-aat1*, *CgCbs*, *CgTyr*, *CgTyrp1* and *CgTyrp2* in mantle by qPCR detection, respectively. The cDNA samples from EGFP-RNAi group (Egfp-i) and *CgB-aat1* and *CgCbs* silencing group (B-aat1-i, Cbs-i) were analyzed by qPCR. The internal gene *ef1 α* of *C. giga* was as control. All data were shown as mean \pm SE ($n=6$). Asterisk (*) was used to indicate the significant difference ($P<0.05$). **c** Protein expressions of *CgB-aat1*, *CgCbs*, *CgTyr*, *CgTyrp1* and *CgTyrp2* in mantle by WB analysis, respectively. GAPDH was used as internal control

Discussion

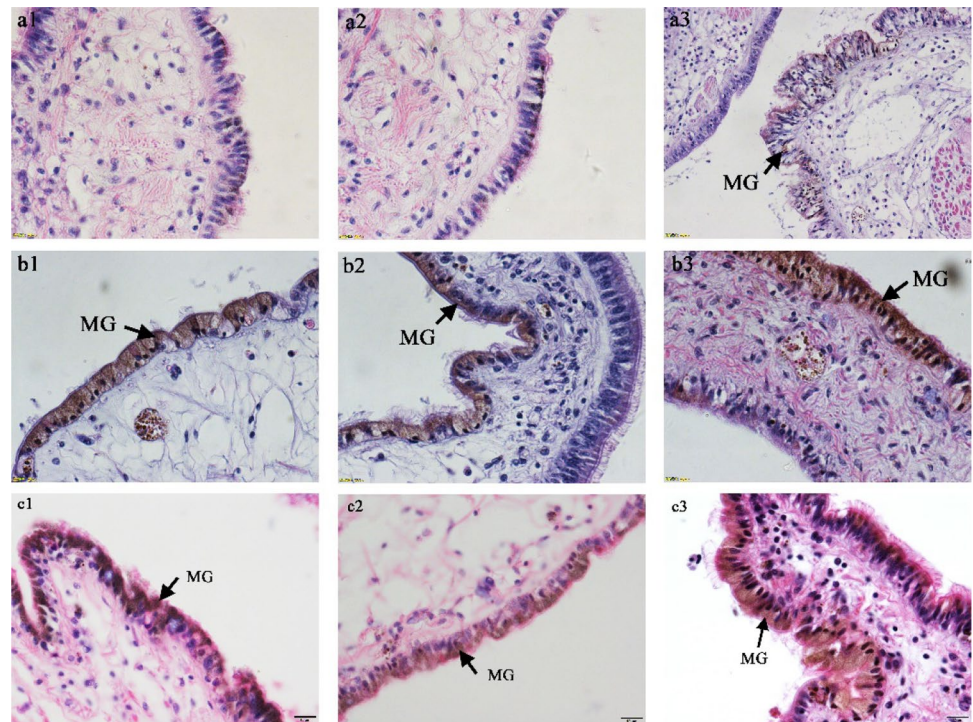
Skin color formation is an important physiological process in the life of organisms. The most abundant pigment is melanin, including eumelanin (brown/black) and pheomelanin (orange/red), have been the main research target in skin pigmentation so far. Previous researches verified that the biosynthesis of pheomelanin is inseparable from the participation of cysteine, which was transported to pigment cells by *Slc7a11*, followed converted to pheomelanin by *Cbs* [1, 9]. It has been identified that *Slc7a11* was an important regulator in pheomelanin production in the skin of mammals [6]. Nevertheless, little is known about the function of *B-aat1* gene in invertebrate and we questioned whether it shares the similar function as *Slc7a11* with regard to melanin synthesis. For this purpose, the deduced *B-aat1* aa sequence possessed typical characteristics, which indicated that the processing of *CgB-aat1* may be similar to *Slc7a11* in other species. Besides, *B-aat1* aa sequence also had several putative transmembrane domains, which was conserved with *Slc7a11* aa sequences in red tilapia [9] and mammals [11–13]. *Cbs* is a downstream gene of *Slc7a11* in pheomelanin biosynthesis and is also the key enzyme in transsulfuration pathway. The catalytic core of *Cbs* consist of a pyridoxal phosphate (PLP) domain containing the active site and CBS domains facilitating allosteric activation by S-adenosylmethionine [26]. Herein, like in other species, the *CgCbs* also include two domains (PALP and CBS), which stabilize the protein structure and enable the protein to play significant biological roles in the conversion of homocysteine to cysteine [27]. These findings indicated that structural and functional of *B-aat1/Cbs* in bivalves might be similar with *Slc7a11/Cbs* in other species.

Knowledge of temporal and tissue-specific expression characteristics of a gene is also worthy for predicting its function. Here, transcriptional level of *CgB-aat1/CgCbs* was both significantly up-regulated after D-veliger larvae and expression of *CgCbs* gene upped to the top at eyed-larva. Because eyed-larvae are the earliest development stage to develop the eye containing the pigment. This result indicated that *CgB-aat1/CgCbs* maybe function in preparation of melanin synthesis at early developmental



stages. Moreover, the maximum expression level of *CgB-aat1/CgCbs* was both observed in central mantle, which acted on secretion of biomineralization proteins and pigmentation in the shell [28]. The gene expression level of *CgB-aat1* was consistently high *Slc7a11* in red tilapia

Fig. 5 Histology of mantle edge in *CgB-aat1* and *CgCbs* silencing groups and control group. **a1–a3** indicated the *CgB-aat1* silencing group, **b1–b3** meant the *CgCbs* silencing group, **c1–c3** indicated the NC group (EGFP silencing group was used as negative control). Compared with NC group, the less brown granules (melanin granules) were observed in mantle edge after *CgB-aat1* interference (a1–a3). And there was no significant change between *CgCbs* silencing group (b1–b3) and NC group (c1–c3). MG: melanin granules. Bars in a1–a3 and b1–b3 were 25 μ m, in c1–c3 were 10 μ m



and mammals [11, 12, 29–31], indicating that *CgB-aat1* may also play an important role in color formation of shell color in mollusks. So far, there has been no report about the cellular location and expression of *CgB-aat1* and *CgCbs* in other mollusks. IF results of *CgB-aat1* and *CgCbs* protein was detected in cytoplasm of epithelial cell and nerve axons in mantle, where they may play vital roles in biochemical synthesis of pheomelanin. The same result was also happened in red tilapia [10]. Gasol et al. [32] discovered that *Slc7a11/xCT* is known as a multi-pass membrane protein, xCT maybe involved in membranous elements composition in the cytoplasm. Moreover, no more information on the cellular location of *B-aat1* and *Cbs* is available in other mollusks.

Feeding of *CgB-aat1*-dsRNA and *CgCbs*-dsRNA resulted in significant down-regulation on *CgB-aat1* and *CgCbs* mRNA as well as protein expression level, respectively. In vertebrate, *Cbs* also play a part in the pheomelanin biosynthesis under the activating of *Slc7a11* expression [33]. Here, *CgCbs* gene expression also significantly suppressed after *CgB-aat1* silencing. Histology result also showed that less brown-granules (melanin granules) were observed in *CgB-aat1* silencing group. Affenzeller et al. [3] identified eumelanin and pheomelanin in *Cepaea nemoralis*. Taken together, the down-regulation of *CgB-aat1* and *CgCbs* maybe reflected that the *CgB-aat1*-*CgCbs* axis in regulating the melanin synthesis pathway (specifically speaking pheomelanin) were existent in the Pacific oyster. However, mass spectrometric investigations for the presence of

eumelanin and pheomelanin in different shell color of the Pacific oyster also need to be studied in the future.

In addition, the expressions result of *Tyrp1* and *Tyrp2* exhibited the lower expression level after *CgCbs* silencing, which is possible to effect melanin formation. *CgTyr* gene expression was also decreased under *CgB-aat1* silencing and significantly down-regulated after *CgCbs* interference. *Tyr* can initiate catalyzed reaction and influence the rate of melanin synthesis [34]. As mentioned earlier, *Tyr* not only participate in eumelanin synthesis but also play an import role in pheomelanin synthesis pathway, in which it initiates biosynthesis of pheomelanin by providing dopaquinone for condensation with cysteine [1]. Combined the histological results, these studies reflected that *CgB-aat1*-*CgTyr*-*CgCbs* axis in pheomelanin regulation pathway maybe also conserved among *C. gigas* and other species, such as insect [35], fish [8, 36] and mammals [37]. Additionally, Emaresi et al. [38] suggested that the *Tyr* gene typically involved in eumelanin synthesis was strongly correlated and negatively associated with the *Slc7a11* and *Cbs* genes typically involved in pheomelanin synthesis in the tawny owl. This research was slightly different with the results in *C. gigas*, indicating function in melanogenesis pathway study between *B-aat1*-*Cbs* and *Tyr* genes need to be research further.

Taken together, *CgB-aat1*-*CgTyr*-*CgCbs* axis maybe responsible for the pheomelanin synthesis and played an important role in mantle pigmentation of *C. gigas*. This finding provides a clue to the melanin pigment mechanisms in bivalves and will be beneficial to bivalve physiology in

shell color formation. Nevertheless, the interplay between the eumelanin and pheomelanin synthesis pathway in *C. gigas* is still a problem that deserves further research.

Supplementary Information The online version contains supplementary material available at <https://doi.org/10.1007/s11033-022-08037-1>.

Acknowledgements This work was supported by the grants from National Natural Science Foundation of China (31972789), the China Agriculture Research System Project (CARS-49), and Earmarked Fund for Agriculture Seed Improvement Project of Shandong Province (2020LZGC016 and 2021LZGC027).

Author contributions QL conceived and designed the study. ZL, BH, LD and CH performed RNA interference experiment and collected the samples. ZL drafted the manuscript and analyzed the data, and QL revised the manuscript. ZL, BH, LD, CH and QL have read and approved the final version of the manuscript.

Declarations

Competing interests The authors declare that they have no known competing financial interests or personal relationships that could have appeared to influence the work reported in this paper.

Ethical approval The Pacific oyster is neither an endangered nor protected species. All experiments in this study were conducted according to national and institutional guidelines.

References

- Barek H, Sugumaran M, Ito S et al (2018) Insect cuticular melanins are distinctly different from those of mammalian epidermal melanins. *Pigment Cell Melan Res* 31(3):384–392. <https://doi.org/10.1111/pcmr.12672>
- Williams ST (2017) Molluscan shell colour. *Biol Rev* 92(2):1039–1058. <https://doi.org/10.1111/brv.12268>
- Affenzeller S, Wolkenstein K, Frauendorf H et al (2019) Eumelanin and pheomelanin pigmentation in mollusc shells may be less common than expected: insights from mass spectrometry. *Front Zool* 16:47–55. <https://doi.org/10.1186/s12983-019-0346-5>
- True JR (2003) Insect melanism: the molecules matter. *Trends Ecol Evol* 18:640–647. <https://doi.org/10.1016/j.tree.2003.09.006>
- Land EJ, Ramsden CA, Riley PA (2004) Quinone chemistry and melanogenesis. *Methods Enzymol* 378:88–109. [https://doi.org/10.1016/S0076-6879\(04\)78005-2](https://doi.org/10.1016/S0076-6879(04)78005-2)
- Chintala S, Li W, Lamoreux ML et al (2005) Slc7a11 gene controls production of pheomelanin pigment and proliferation of cultured cells. *Proc Natl Acad Sci USA* 102(31):10964–10969. <https://doi.org/10.1073/pnas.0502856102>
- Jiang Y, Zhang SH, Xu J et al (2014) Comparative transcriptome analysis reveals the genetic basis of skin color variation in common carp. *PLoS ONE* 9(9):e108200. <https://doi.org/10.1371/journal.pone.0108200>
- Luo MK, Lu GQ, Yin HR et al (2021) Fish pigmentation and coloration: molecular mechanisms and aquaculture perspectives. *Rev Aquac*. <https://doi.org/10.1111/raq.12583>
- Zhu W, Tian CX, Huang Y et al (2016) Comparative transcriptome analysis identifies candidate genes related to skin color differentiation in Red tilapia. *Sci Rep* 6:31347. <https://doi.org/10.1038/srep31347>
- Wang LM, Bu HY, Song FB et al (2019) Characterization and functional analysis of *slc7a11* gene, involved in skin color differentiation in the red tilapia. *Comp Biochem Physiol A*. <https://doi.org/10.1016/j.cbpa.2019.110529>
- Tian X, Meng XL, Wang LY et al (2015) Molecular cloning, mRNA expression and tissue distribution analysis of *Slc7all* gene in alpaca (*Lama paco*) skins associated with different coat colors. *Gene* 555:88–94. <https://doi.org/10.1016/j.gene.2014.10.029>
- He X, Li HT, Zhou ZY et al (2012) Production of brown/yellow patches in the SLC7A11 transgenic sheep via testicular injection of transgene. *J Genet Genom* 39(6):281–285. <https://doi.org/10.1016/j.jgg.2012.04.005>
- Yang NS, Liu M, Zhao BH et al (2018) RNAi-mediated *SLC7A11* knockdown inhibits melanogenesis-related genes expression in rabbit skin fibroblasts. *J Genet* 97(2):463–468. <https://doi.org/10.1007/s12041-018-0945-5>
- Romero I, Tellez J, Yamanaka LE et al (2014) Transsulfuration is an active pathway for cysteine biosynthesis in *Trypanosoma rangeli*. *Parasites Vectors* 7:197. <https://doi.org/10.1186/1756-3305-7-197>
- Lemer S, Saulnier D, Gueguen Y et al (2015) Identification of genes associated with shell color in the black-lipped pearl oyster *Pinctada margaritifera*. *BMC Genom* 16:568. <https://doi.org/10.1186/s12864-015-1776-x>
- Yu FF, Qu BL, Lin DD et al (2018) Pax3 gene regulated melanin synthesis by tyrosinase pathway in *Pteria penguin*. *Int J Mol Sci* 19:3700. <https://doi.org/10.3390/ijms19123700>
- Zhang SJ, Wang HX, Yu JJ et al (2018) Identification of a gene encoding microphthalmia-associated transcription factor and its association with shell color in the clam *Meretrix petechialis*. *Comp Biochem Physiol B* 225:75–83. <https://doi.org/10.1016/j.cbpb.2018.04.007>
- Han ZQ, Li Q, Liu SK et al (2019) Genetic variability of an orange-shell line of the Pacific oyster *Crassostrea gigas* during artificial selection inferred from microsatellites and mitochondrial COI sequences. *Aquaculture* 508:159–166. <https://doi.org/10.1016/j.aquaculture.2019.04.074>
- Li ZZ, Li Q, Liu SK et al (2021) Integrated analysis of coding genes and non-coding RNAs associated with shell color in the Pacific oyster (*Crassostrea gigas*). *Mar Biotechnol* 23:417–429. <https://doi.org/10.1007/s10126-021-10034-7>
- Feng DD, Li Q, Yu H (2019) RNA interference by ingested dsRNA-expressing bacteria to study shell biosynthesis and pigmentation in *Crassostrea gigas*. *Mar Biotechnol* 21:526–536. <https://doi.org/10.1007/s10126-019-09900-2>
- Li ZZ, Li Q, Xu CX et al (2022) Molecular characterization of *Pax7* and its role in melanin synthesis in *Crassostrea gigas*. *Comp Biochem Physiol B*. <https://doi.org/10.1016/j.cbpb.2022.110720>
- Du YS, Zhang LL, Xu F et al (2013) Validation of housekeeping genes as internal controls for studying gene expression during Pacific oyster (*Crassostrea gigas*) development by quantitative real-time PCR. *Fish Shellfish Immunol* 34:939–945. <https://doi.org/10.1016/j.fsi.2012.12.007>
- Livak KJ, Schmittgen TD (2001) Analysis of relative gene expression data using real-time quantitative PCR and the 2(T) (-Delta Delta C) method. *Methods* 25:402–408. <https://doi.org/10.1006/meth.2001.1262>
- Liu HF, Wang J, Zhang LM et al (2021) Effects of recombinant AMH during oocyte maturation in spotted steed *Hemibarbus maculatus*. *Aquaculture* 543:736961. <https://doi.org/10.1016/j.aquaculture.2021.736961>
- Li YJ, Ren LT, Fu HR et al (2021) Crosstalk between dopamine and insulin signaling in growth control of the oyster. *Gen Comp Endocr* 313:113895. <https://doi.org/10.1016/j.ygcen.2021.113895>
- Koutmos M, Kabil O, Smith JL et al (2010) Structural basis for substrate activation and regulation by cystathionine

- beta-synthase (CBS) domains in cystathionine β -synthase. PNAS 107(49):20958–20963. <https://doi.org/10.1073/pnas.1011448107>
27. Giménez-Mascarell P, Majtan T, Oyenarte I et al (2018) Crystal structure of cystathionine β -synthase from honeybee *Apis mellifera*. J Struct Biol 202(1):82–93. <https://doi.org/10.1016/j.jsb.2017.12.008>
 28. Addadi L, Joester D, Nudelman F et al (2006) Mollusk shell formation: a source of new concepts for understanding biomineralization processes. Chem Eur J 12(4):980–987. <https://doi.org/10.1002/chem.200500980>
 29. Li HT, He X, Zhou ZY et al (2012) Expression levels of Slc7a11 in skin of kazakh sheep with different coat color. Hereditas 34:1314–1319. <https://doi.org/10.3724/sp.j.1005.2012.01314>
 30. Li SJ, Wang C, Yu WH et al (2012) Identification of genes related to white and black plumage formation by RNA-Seq from white and black feather bulbs in ducks. PLoS ONE 7:e36592. <https://doi.org/10.1371/journal.pone.0036592>
 31. Sato H, Tamba M, Kuriyama-Matsumura K et al (2000) Molecular cloning and expression of human xCT, the light chain of amino acid transport system xc⁻. Antioxid Redox Signal 2:665–671. <https://doi.org/10.1089/ars.2000.2.4-665>
 32. Gasol E, Jimenez-vidal M, Chillaron J et al (2004) Membrane topology of system xc⁻ light subunit reveals a re-entrant loop with substrate restricted accessibility. J Biol Chem 279(30):31228–31236. <https://doi.org/10.1074/jbc.M402428200>
 33. Hoekstra HE (2006) Genetics, development and evolution of adaptive pigmentation in vertebrates. Heredity 97:222–234. <https://doi.org/10.1038/sj.hdy.6800861>
 34. Busca R, Ballotti R (2000) Cyclic AMP a key messenger in the regulation of skin pigmentation. Pigment Cell Res 13:60–69. <https://doi.org/10.1034/j.1600-0749.2000.130203.x>
 35. Sugumaran M (2009) Complexities of cuticular pigmentation in insects. Pigment Cell Melan Res 22(5):523–525. <https://doi.org/10.1111/j.1755-148x.2009.00608.x>
 36. Fang WY, Huang JR, Li SZ et al (2022) Identification of pigment genes (melanin, carotenoid and pteridine) associated with skin color variant in red tilapia using transcriptome analysis. Aquaculture 547:737429. <https://doi.org/10.1016/j.aquaculture.2021.737429>
 37. Morgan AM, Lo J, Fisher DE (2013) How does pheomelanin synthesis contribute to melanomagenesis? Two distinct mechanisms could explain the carcinogenicity of pheomelanin synthesis. Bioessays 35(8):672–676. <https://doi.org/10.1002/bies.201300020>
 38. Emaresi G, Ducrest AL, Bize P et al (2013) Pleiotropy in the melanocortin system: expression levels of this system are associated with melanogenesis and pigmentation in the tawny owl (*Strix aluco*). Mol Ecol 22(19):4915–4930. <https://doi.org/10.1111/mec.12438>

Publisher's Note Springer Nature remains neutral with regard to jurisdictional claims in published maps and institutional affiliations.

Springer Nature or its licensor (e.g. a society or other partner) holds exclusive rights to this article under a publishing agreement with the author(s) or other rightsholder(s); author self-archiving of the accepted manuscript version of this article is solely governed by the terms of such publishing agreement and applicable law.